

# Temperature and Silicon Film Thickness Influence on the Operation of Lateral SOI PIN Photodiodes for Detection of Short Wavelengths

Michelly de Souza<sup>1</sup>, Olivier Bulteel<sup>2</sup>, Denis Flandre<sup>2</sup>, and Marcelo A. Pavanello<sup>1</sup>

<sup>1</sup>Electrical Engineering Department, Centro Universitário da FEI, São Bernardo do Campo, Brazil

<sup>2</sup>Laboratoire de Microélectronique, ICTEAM Institute, UC Louvain, Louvain-la-Neuve, Belgium  
e-mail: michelly@fei.edu.br

## ABSTRACT

This work presents an analysis of the temperature influence on the performance of a lateral thin-film SOI PIN photodiodes when illuminated by low wavelengths, in the range of blue and ultra-violet (UV). Experimental measurements performed from 100K to 400K showed that the optical responsivity of SOI PIN photodetectors is affected by temperature change, being reduced at low and moderately high temperatures. Two-dimensional numerical simulations showed the same trends as in the experimental results, and were used both to investigate the physical phenomena responsible for the observed behavior as a function of the temperature as well as to predict the influence of silicon film thickness down-scaling on the photodetector performance.

**Index Terms:** Silicon-on-insulator, PIN diodes, Photodetector, Temperature.

## INTRODUCTION

The incidence of light in a semiconductor device promotes carriers generation, which can contribute to the device current if the hole-electron pairs do not recombine, but are quickly separated by the action of an electric field. Taking advantage of this effect, PN junctions are often used as photodetectors. In these devices, electron-hole pairs are generated by the incidence of photons and contribute to increase the diode reverse current.

The width of the depleted region is then a trade-off between speed and sensitivity, i.e. it must be large enough to allow for the absorption of a significant number of incident photons, which will generate carriers to contribute for the increase of photocurrent, but sufficiently short to reduce the transit time for drift of photogenerated carriers [1, 2]. A common way to control the depleted region width is to use PIN photodiodes [1]. PIN diodes consist of PN junctions separated by an intrinsic (I) region [1] with length  $L_i$ , which, in practice, may correspond to either a P-type or N-type region with low doping level.

Optical detection at short wavelengths close to blue and UV ( $\lambda < 480$  nm) have many applications in biomedical and environmental fields such as for DNA concentration measurement, bacteria and protein detection, and ultraviolet and ozone rates measurements [3]. In addition, high density DVDs use a blue wavelength of 405 nm, allowing increased storage

capacity [4]. The absorption of light in semiconductors varies according to its thickness. Silicon devices absorb light as a function of their thickness for wavelengths ( $\lambda$ ) up to 1100 nm [1]. Specifically for the blue light, the absorption takes place near to the surface in silicon. For instance, for  $\lambda = 400$  nm the absorption depth is close to 0.1  $\mu\text{m}$  [1, 4]. In this case, the remaining silicon substrate which is not used for photodetection, only contributes to increase dark current due to thermal carrier generation [5].

An efficient alternative to absorb short wavelengths with Si-based devices is to implement photodetectors in thin silicon layers based on SOI wafers [4]. With this purpose, lateral PIN photodiodes can be easily obtained using a standard SOI CMOS standard process flow. Thanks to the thin silicon film and the isolation promoted by the presence of the buried oxide, these devices exhibit very low dark current, high quantum efficiency and responsivity, which make them suitable for high speed applications [4]. In addition, it allows for the co-integration with CMOS circuitry.

This paper presents an analysis of the operation of lateral thin-film SOI PIN photodiodes for the detection of short wavelengths, in the range of blue and ultra-violet (UV), in a wide temperature range, reaching the cryogenic regime. Experimental measurements were performed from 100 K to 400 K and two-dimensional numerical simulations were used to investigate the physical phenomena responsible for the

## Temperature and Silicon Film Thickness Influence on the Operation of Lateral SOI PIN Photodiodes for Detection of Short Wavelengths

Souza, Bulteel, Flandre & Pavanello

measured characteristics in the entire temperature range. In addition, by using numerical simulations, the thin silicon film had its thickness reduced, with the purpose of predicting the performance of this photodetector in more advanced technologies.

### PHOTODIODES CHARACTERISTICS

Lateral interdigitated PIN diodes were implemented in a SOI wafer following the process described in [6]. After processing, the thin-film silicon layer ( $t_{Si}$ ) features 80 nm, separated from the substrate by a buried oxide ( $t_{oxb}$ ) of 390 nm of thickness. Additionally, a thick silicon oxide layer, and an anti-reflection coating (ARC) of alumina ( $Al_2O_3$ ) of 50 nm ( $t_{ARC}$ ) covers all devices. The intrinsic region of the PIN diodes is actually a p-type lightly doped, keeping the natural wafer doping concentration. The devices thicknesses and doping concentration levels are summarized in Table I.

Figure 1 presents a schematic cross-section of one finger of a PIN photodiode studied in this work, indicating thicknesses and other important dimensions.

**Table I.** Lateral SOI PIN technological parameters.

Parameter	
Silicon film thickness, $t_{Si}$	80 nm
Buried oxide thickness, $t_{oxb}$	390 nm
Passivation oxide thickness, $t_{ox}$	280 nm
Anti-reflection coating thickness, $t_{ARC}$	50 nm
Intrinsic region doping concentration, $N_I$	$1 \times 10^{15} \text{ cm}^{-3}$
P region doping concentration, $N_A$	$1 \times 10^{20} \text{ cm}^{-3}$
N region doping concentration, $N_D$	$4 \times 10^{20} \text{ cm}^{-3}$

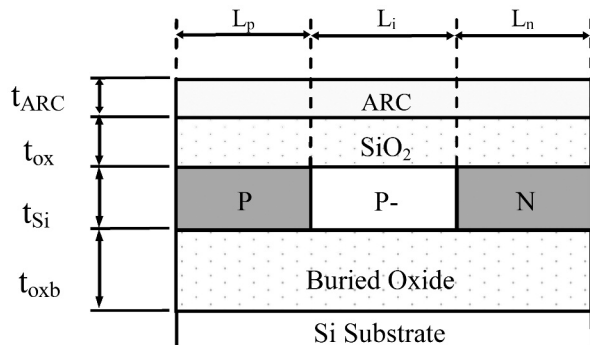


**Figure 1.** Cross-section of one finger of an interdigitated PIN SOI lateral photodiode

The length of the intrinsic region ( $L_i$ ) is a key parameter in the design of a PIN diode [4]. While a small intrinsic region could be desired, aiming to increase collection of electron-hole pairs by reducing the generated electrons-holes recombination, it would also increase the dark current, due to the increase in the number of fingers for a fixed total area. However, by enlarging the intrinsic region, aiming to reduce the

number of fingers and therefore dark current, the electron-hole recombination increases, causing the photo-generated current to decrease. For the present technology, it has been found that the best compromise between dark and photogenerated current is obtained for PIN diodes with  $L_i$  around 18  $\mu\text{m}$ . This corresponds to the diffusion length of the carriers with an effective lifetime of 0.1  $\mu\text{s}$  at room temperature in this technology [4]. However in this case, diodes with intrinsic length of 8  $\mu\text{m}$  and 9  $\mu\text{m}$  were used, aiming to reduce the recombination. Regarding the length of the highly doped P and N regions,  $L_{p,n}$ , it must be as small as possible, aiming to maximize the intrinsic region area, allowing to enhance the depleted zone and thus increasing the generated photocurrent. However, their minimum length is limited by the technology, which in this case is 9  $\mu\text{m}$ , considering the contact and metal interconnections minimum dimensions.

For this analysis, two interdigitated lateral PIN diodes were characterized. The dimensions of the measured devices are presented in Table II.

**Table II.** Dimensions of the measured SOI PIN photodiodes.

Intrinsic length, $L_i$	Total width, W	Total Area	P, N regions length, $L_{p,n}$
8 $\mu\text{m}$	14.5 mm	0.25 mm <sup>2</sup> (500 $\mu\text{m}$ x 500 $\mu\text{m}$ )	9 $\mu\text{m}$
9 $\mu\text{m}$	55.0 mm	1 mm <sup>2</sup> (1 mm x 1 mm)	

Figure 2 presents an optical microscope image of part of an interdigitated PIN SOI lateral photodiode measured.

### EXPERIMENTAL MEASUREMENT RESULTS

With the purpose of evaluating the performance of PIN diodes as photodetectors in a wide temperature range, the devices were measured for temperatures ( $T$ ), ranging from 100 K up to 400 K. The temperature has been controlled by using the Variable Temperature Micro Probe System from MMR Technologies [7]. For the electrical characterization, the substrate has been grounded and the diode current ( $I_D$ ) measured as a function of the applied voltage bias ( $V_D$ ) using an Agilent 4156C Semiconductor Parameter Analyzer, both in the absence of light and when illuminated with different wavelengths ( $\lambda$ ), ranging from 397 nm (near UV) to 461 nm (blue).

The absolute current as a function of the applied voltage, measured for the photodiode with  $L_i=9\mu\text{m}$ , in the absence of light, is presented in Figure 3, for temperatures ranging from 100 K to 400 K. As presented in this figure, the rise of temperature increases the dark current ( $I_{DARK}$ ) in several orders of magnitude, as a result of increased thermal generation of electrons [2].

Temperature and Silicon Film Thickness Influence on the Operation of Lateral SOI PIN Photodiodes for Detection of Short Wavelengths  
Souza, Bulteel, Flandre & Pavanello

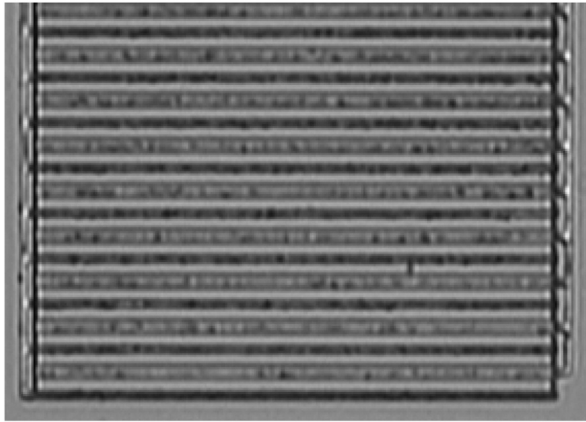


**Figure 2.** Optical microscope top view of an interdigitated PIN SOI lateral photodiode measured in this work.

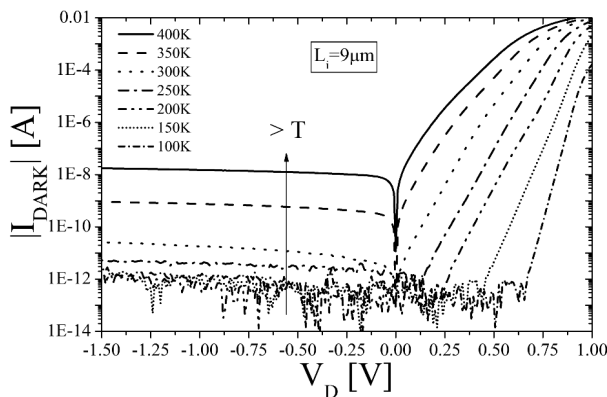


**Figure 3.** Absolute dark current as a function of applied voltage for a PIN photodiode with  $L_i=9\ \mu\text{m}$ , measured at different temperatures.

Figure 4 presents the dark current of the diode with  $L_i=8\ \mu\text{m}$  and smaller area. By comparing the curves presented in Figures 3 and 4, one can note that the dark current level is higher in the diode with larger  $W$ . In order to account for this difference, the absolute dark current has been normalized by the total width ( $|I_{\text{DARK}}/W|$ ) and is presented in Figure 5, as a function of the temperature, for different  $V_D$  values in the range between  $-0.75\text{V}$  and  $-1.5\text{V}$ .

As presented by the results in Figure 5, there is no significant difference between the normalized dark current of both diodes, indicating that the width does not play an important role in  $I_{\text{DARK}}$  and any difference caused by the different intrinsic lengths is not observable. In addition,  $V_D$  barely influences the dark current, which is rather stable with reverse bias, as can be also seen in the  $|I_{\text{DARK}}|$  vs  $V_D$  curves in Figures 3 and 4.

The presented results also show that  $I_{\text{DARK}}$  reduces exponentially as the temperature is lowered. However, this reduction can only be clearly seen down to 250 K. Below this temperature the dark current cannot be measured, due to limitations of the experimental setup, which is not capable of measuring current levels lower than tenths of pA. For the photode-

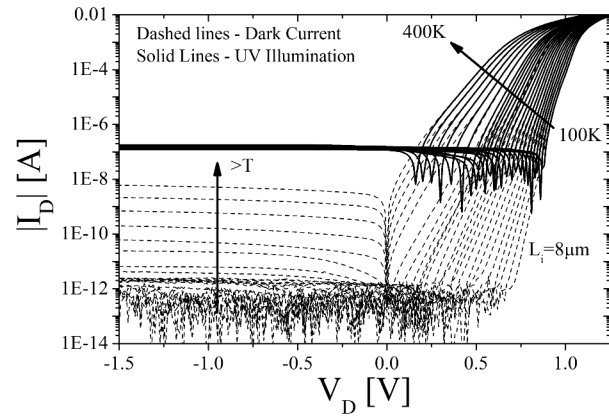


**Figure 4.** Dark current and photodiode current under UV illumination, measured at different temperatures, at  $\lambda=397\ \text{nm}$ .

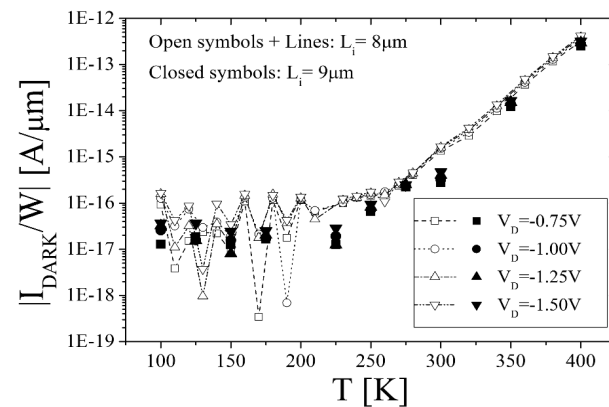


**Figure 5.** Dark current normalized by the width as a function of the temperature for photodiodes with  $L_i=8\ \mu\text{m}$  and  $9\ \mu\text{m}$ , for different  $V_D$  values.

tor operation, the dark current must be kept as small as possible, as it acts as noise. Therefore, the observed  $I_{\text{DARK}}$  reduction suggests that higher signal-to-noise ratio can be obtained for PIN photodiodes operating at cryogenic regime.

Figure 4 also presents the photogenerated current under near UV illumination ( $\lambda=397\ \text{nm}$ ). Apart from presenting higher values, it is clearly seen that in comparison to the dark current, that varies several orders of magnitude with temperature increase, the reverse photodiode current under illumination is not strongly temperature dependent. As in the case of  $I_{\text{DARK}}$ , the current generated by the incidence of light has shown to be larger in the diode with  $L_i=9\ \mu\text{m}$  due to larger photosensitive area [7]. Therefore, for comparison purposes, the photogenerated current ( $I_D$ ) has been also normalized by the device width and is presented in Figure 6 as a function of temperature for different values of reverse applied voltage, under UV illumination ( $\lambda=397\ \text{nm}$ ). Even if the differences in width are taken into account, the photodiode with larger  $L_i$  presents higher current level under illumination, owing to the larger area for photons absorption (intrinsic region). Despite the differences in the cur-

## Temperature and Silicon Film Thickness Influence on the Operation of Lateral SOI PIN Photodiodes for Detection of Short Wavelengths

Souza, Bulteel, Flandre & Pavanello

rent level, the  $I_D/W$  variation with temperature presents the same tendency, independently of the device intrinsic length. According to the results in Figure 6, the current generated by the incidence of short wavelengths suffers a decrease both at low and high temperatures and presents a maximum around 275 K.

Differently from the dark current, which showed to be independent of the applied  $V_D$ , the photogenerated current at high temperatures is affected by the applied voltage. On the other hand,  $V_D$  has negligible effect on the photogeneration of current for temperatures below 250 K.

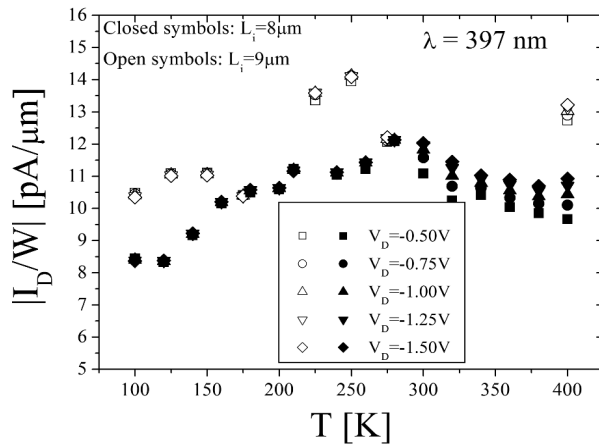


**Figure 6.** Normalized photogenerated current as a function of the temperature for photodiodes featuring  $L_i=8\ \mu\text{m}$  and  $9\ \mu\text{m}$ , extracted at different values of  $V_D$ , under UV illumination ( $\lambda=397\ \text{nm}$ ).

Similar trend has been obtained when photodiodes were illuminated by blue and violet light, as shown in Figure 7. This figure presents  $|I_D/W|$  vs  $T$  curves measured for the photodiode with  $L_i=8\ \mu\text{m}$  under blue and violet lights, with different wavelengths and luminous intensities, at  $V_D=-1.0\text{V}$  and  $-1.5\text{V}$ . In these curves it is possible to note that  $I_D$  increases at higher temperatures, giving rise to a valley in the  $I_D/W$  vs  $T$  curves around  $T=350\ \text{K}$ .

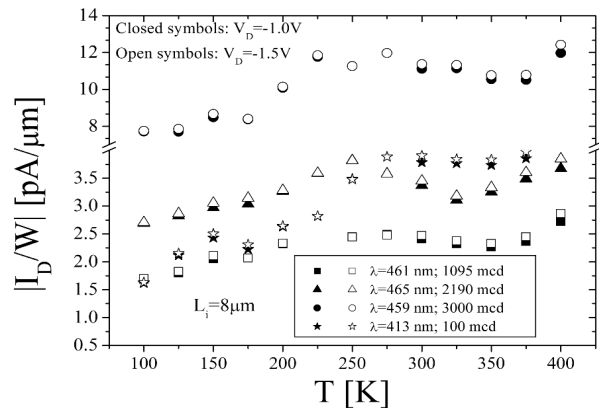


**Figure 7.** Absolute normalized photocurrent  $|I_D/W|$  as a function of the temperature, for the diode with  $L_i=8\ \mu\text{m}$ , illuminated with blue ( $\lambda=459\ \text{nm}$ ,  $461\ \text{nm}$  and  $465\ \text{nm}$ ) and violet ( $\lambda=413\ \text{nm}$ ) light with different luminous intensities.

## NUMERICAL SIMULATION ANALYSIS

Aiming to investigate the physical phenomena related to the observed experimental results and extend the analysis for more advanced technologies, with reduced silicon film thickness, two-dimensional numerical simulations of thin-film SOI PIN photodiodes were performed with Atlas software [8].

All devices were simulated considering a steep transition of the doping concentration at the boundary of P, intrinsic and N regions and using the same technological parameters as the experimental samples ( $t_{\text{Si}}=80\ \text{nm}$ ,  $t_{\text{oxb}}=390\ \text{nm}$ ,  $N_A=1\times 10^{20}\ \text{cm}^{-3}$ ,  $N_{\text{intrinsic}}=1\times 10^{15}\ \text{cm}^{-3}$  and  $N_D=4\times 10^{20}\ \text{cm}^{-3}$ ), with  $L_i=8\ \mu\text{m}$ . For the simulated devices, no ARC has been included.

Physical models accounting for mobility ( $\mu$ ) dependence on doping concentration ( $N$ ), temperature and electric field, bandgap narrowing (BGN), Auger and SRH recombination, doping and temperature-dependent lifetime and incomplete carrier ionization for the lightly doped region were included in the simulation files. It is worthwhile noting that no optimization of model parameters has been made, which is beyond the scope of this analysis and may affect the quantitative results but does not affect the qualitative analysis. Illumination sources with blue ( $\lambda=460\ \text{nm}$ ), violet ( $\lambda=410\ \text{nm}$ ) and UV ( $\lambda=390\ \text{nm}$ ) wavelengths were considered, all with power density of optical beam of  $1\ \text{mW}/\text{cm}^2$ .

### A. Physical phenomena related to temperature variation

Curves of current as a function of the applied voltage, similar to those presented in Figure 4 were simulated for temperatures ranging between 100 K and 400 K, and under the incidence of different wavelengths. From these curves, the current as a function of the temperature has been extracted and is presented in Figure 8.

As shown in this figure, the simulated  $I_D/W$  curves present the same tendency with temperature as the measured data suggesting that the selected set of physical models is able to describe the experimental photodiode behaviour. It is worthwhile mentioning that despite having the same power, UV illumination results in larger photogeneration of carriers than blue and violet ones. This effect is attributed to the silicon thickness used in these simulations, which yields larger responsivity for  $\lambda$  around 400 nm in comparison to 470 nm [4]. In the presented curves, the current generated by the incidence of UV light is approximately 2.64 and 1.42 times larger than for the blue and violet ones, respectively, in the entire temperature range. In order to identify the physical phenomena responsible for the photocurrent variation with tem-

**Temperature and Silicon Film Thickness Influence on the Operation of Lateral SOI PIN Photodiodes for Detection of Short Wavelengths**  
 Souza, Bulteel, Flandre & Pavanello

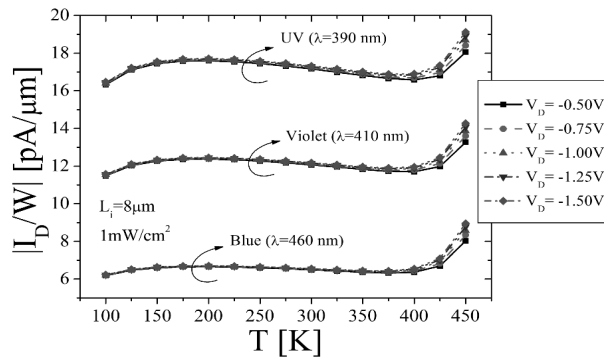


**Figure 8.** Simulated  $I_D/W$  as a function of the temperature, for a PIN photodiode with  $L_i=8 \mu\text{m}$ , illuminated with UV, violet and blue light with incident power of  $1 \text{ mW}/\text{cm}^2$ .

perature, simulations were performed with different sets of physical models, considering  $\lambda=390 \text{ nm}$ . The results are presented in Figure 9.

In this figure, the curve represented by closed squares corresponds to the current obtained by using the complete set of models described and used to obtain the curves in Figure 8, while the open triangles represent the current simulated neglecting all the physical phenomena mentioned before. In this case, if none of these effects were considered, quasi-constant  $I_D$  vs  $T$  curves are obtained. As shown through the curve with open diamonds, where no mobility or bandgap narrowing effects are taken into account yet, the current level and its increase at higher temperatures are related to the carrier lifetime dependence on doping concentration and temperature. However, if only this effect is taken into account, the photogenerated curve shows to increase at low temperatures, apart from being virtually constant at moderate temperatures, which disagrees with the measured data.

However, if the bandgap narrowing effect is added to the simulation (open stars), a reduction of  $I_D$  is obtained at low temperatures, since BGN in the highly doped P and N regions becomes more pronounced with temperature lowering [9]. This effect

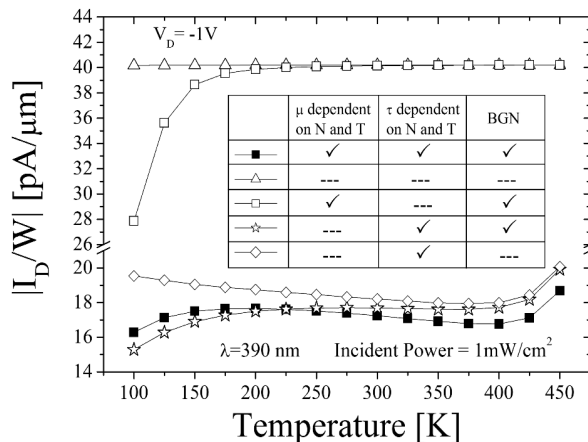


**Figure 9.** Simulated  $I_D/W$  vs  $T$  curves, considering  $\lambda=390 \text{ nm}$  with incident power of  $1 \text{ mW}/\text{cm}^2$  and different sets of models.

can be also noted by the curve represented in open squares, that has been obtained neglecting only the effect of lifetime dependence on N and T.

Finally, the  $I_D$  reduction observed at moderately high temperatures is related to the mobility degradation caused by the temperature increase. On the contrary, the mobility improvement at cryogenic temperatures, partly compensates the current reduction caused by the bandgap narrowing, as can be noted through the comparison of the curves represented by stars and closed squares.

**B. Silicon film thickness influence on the operation of SOI PIN Photodiodes**

As the use of lateral SOI PIN diodes allow to implement photodetectors integrated with CMOS circuits, it is important to know the behavior of these devices for the implementation of photodetectors in more advanced technologies, where the silicon film thickness is reduced. With this purpose, two sets of technological parameters were also used to simulate the photodiodes. The first one features  $t_{Si}=40 \text{ nm}$  and  $t_{oxb}=145 \text{ nm}$ , as in the 150 nm technology from Oki Semiconductors [10] and the second one,  $t_{Si}=15 \text{ nm}$  and  $t_{oxb}=150 \text{ nm}$ , following the 65 nm technology from IMEC [11]. The lengths and doping concentrations for P, N and intrinsic regions were kept as in the previous simulations.

Figure 10 presents the dark current as a function of the temperature, obtained for the three different silicon film thicknesses. Due to numerical precision limitations, the simulator, very low current levels are subjected to significant numerical noise [8]. For this reason, it was not possible to simulate the dark current of these devices for low temperatures.

Therefore, it was not possible to predict the dark current below room temperature, as can be seen in the presented curves. However, for high temperatures the dark current presented the same increasing tendency and little dependence on the applied vol-

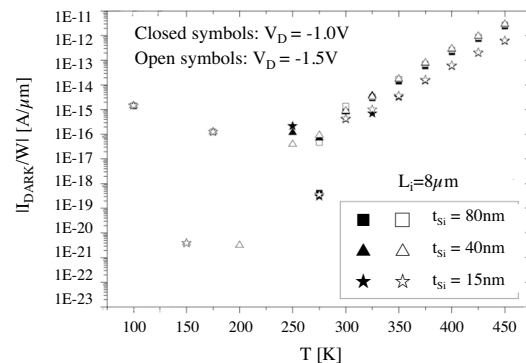


**Figure 10.** Simulated dark current as a function of the temperature for photodiodes with  $L_i=8 \mu\text{m}$ , with different silicon film thicknesses, extracted at  $V_D = -1.0\text{V}$  and  $-1.5\text{V}$ .

## Temperature and Silicon Film Thickness Influence on the Operation of Lateral SOI PIN Photodiodes for Detection of Short Wavelengths

Souza, Bulteel, Flandre & Pavanello

tage, as observed in the experimental curves shown in Figure 5. The presented results also allow for noting that there is a reduction of  $I_{DARK}$  for very thin silicon film device in comparison to thicker ones.

Figure 11 presents the obtained current for the three simulated silicon film thicknesses as a function of the temperature, for  $\lambda=460$  nm (blue), 410 nm (violet) and 390 nm (ultra-violet), extracted at  $V_D = -1.0V$ . The simulated results show that by thinning the silicon film down, the photogenerated current decreases, as a consequence of the reduction of the amount of absorbed photons, independently on the incident wavelength.

From the results in Figure 11 and aiming to verify the influence of the silicon film thickness in the selectivity of the photodetector to the studied wavelengths, the ratio between the current generated by UV and blue/violet light, at  $V_D=-1V$ , for temperatures ranging from 100K to 400K, has been obtained and is presented in Table III.

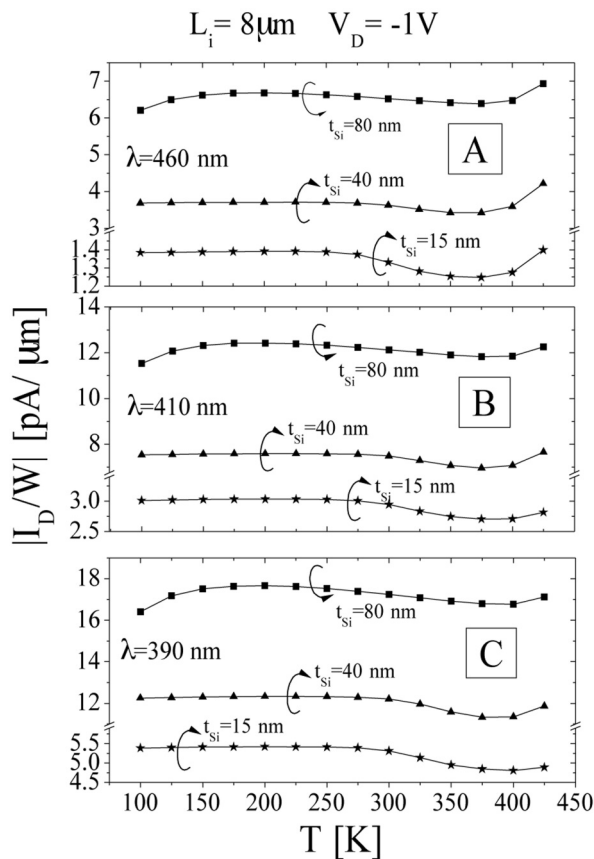


**Figure 11.** Simulated  $I_D/W$  as a function of the temperature, for a PIN photodiode with  $L_i=8 \mu\text{m}$  and different silicon film thickness, illuminated with blue (A), violet (B) and ultra-violet (C) light with incident power of  $1 \text{ mW/cm}^2$ .

**Table III.** Ratio  $[(I_D/W)_{UV} / (I_D/W)_{VIOLET}]$  and  $[(I_D/W)_{UV} / (I_D/W)_{BLUE}]$  extracted from the curves simulated from 100K to 400K at  $V_D=-1V$ .

$t_{Si}$ [nm]	$(I_D/W)_{UV} / (I_D/W)_{VIOLET}$	$(I_D/W)_{UV} / (I_D/W)_{BLUE}$
15	$1.792 \pm 0.010$	$3.906 \pm 0.057$
40	$1.627 \pm 0.008$	$3.324 \pm 0.057$
80	$1.421 \pm 0.002$	$2.637 \pm 0.015$

Reference [4] reports that for  $t_{Si}$  around 80 nm, the responsivity for UV light is from 2 to 3 times larger than for the blue one. The simulated results showed that this selectivity increases with silicon film thickness reduction, despite of the photocurrent reduction observed in Figure 11. The photodiodes sensitivity to UV light becomes larger in comparison to blue and violet ones, increasing from 2.64 times to around 3.91 times larger when reducing  $t_{Si}$  from 80 nm to 15 nm, with  $\lambda=460\text{nm}$ , and from 1.42 times to 1.79 times with  $\lambda=410\text{nm}$  and the same  $t_{Si}$  range.

Figure 12 presents the photodiode current normalized by its room temperature (300K) value. These curves show that as the silicon film is thinned down, the current under illumination becomes less sensitive to temperature reduction, mainly below 250K. On the other hand, the current decrease with temperature rise becomes more pronounced, as an effect of mobility reduction due to the thinning of the silicon film.

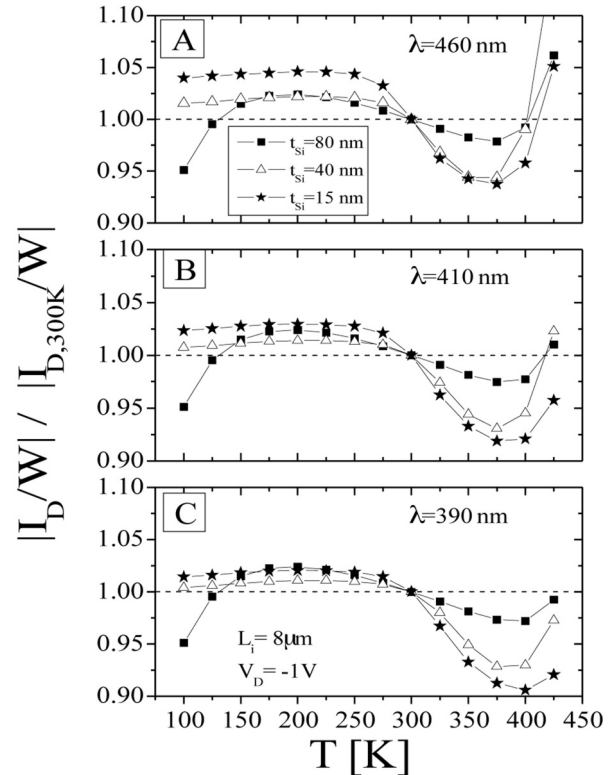


**Figure 12.**  $I_D/W$  normalized by its room-temperature value as a function of the temperature, for different silicon film thickness, illuminated with blue (A), violet (B) and ultra-violet (C) light with incident power of  $1 \text{ mW/cm}^2$ .

## CONCLUSIONS

In this work the influence of the temperature on the performance of lateral SOI PIN diodes for the detection of short wavelengths, in the range of blue and ultra-violet, has been presented. Experimental results showed that the current generated by these wavelengths incidence reduces both at cryogenic and

**Temperature and Silicon Film Thickness Influence on the Operation of Lateral SOI PIN Photodiodes for Detection of Short Wavelengths**  
 Souza, Bulteel, Flandre & Pavanello

moderately high temperatures, reaching a maximum value around 250K–300K. Further temperature increase is responsible for causing another current rise. The dark current is significantly reduced by the temperature lowering, indicating that these photodetectors are able to provide higher signal-to-noise ratio in the cryogenics regime.

Two-dimensional numerical simulations were used to reproduce the experimental results and showed that the current reduction observed in the cryogenic regime is caused by the bandgap narrowing effect in the highly doped regions, which becomes more pronounced with temperature reduction. On the other hand, the photocurrent increase at high temperatures is related to the doping and temperature dependence of carriers lifetime. Numerical simulations were also performed in order to extend the experimental analysis to thinner silicon film technologies. The simulated results indicate that the silicon film thickness reduction causes both a decrease of the photogenerated current, but also higher selectivity between UV and blue/violet wavelengths.

#### ACKNOWLEDGEMENTS

M. de Souza and M. A. Pavanello acknowledge to the Brazilian research-funding agencies CAPES, FAPESP and CNPq for the financial support to this work. This work has been partially supported by the

international cooperation project Brazil-Belgium funded by CNPq and FNRS.

#### REFERENCES

1. S. M. Sze, *Physics of Semiconductor Devices*, John Wiley and Sons, New York: 1981, pages 743-760.
2. B. G. Streetman and S. Banerjee, *Solid State Electronic Devices*, Prentice Hall, New Jersey: 2000, pages 384-385.
3. O. Bulteel and D. Flandre, "Optimization of blue/UV sensors using p-i-n photodiodes in thin-film SOI technology", *ECS Transactions*, vol. 19, n. 4, 2009, pages 175-180.
4. A. Afzalian and D. Flandre, "Physical modeling and design of thin-film SOI lateral PIN photodiodes", *IEEE Trans. On Electron Devices*, vol. 52, n. 6, 2005, pages 1116-1122.
5. H. Zimmermann, B. Muller, A. Hammer, K. Herzog, P. Seegebrecht, "Large-area lateral p-i-n photodiode on SOI", *IEEE Trans. On Electron Devices*, vol. 49, n. 2, 2002, pages 334-336.
6. D. Flandre et al, "Fully depleted SOI CMOS technology for hetero-geneous micropower, high-temperature or RF Microsystems", *Solid-State Electronics*, v. 45, no. 4, April, 2001, pages 541-549.
7. M. de Souza, O. Bulteel, D. Flandre and M. A. Pavanello, "Analysis of Lateral SOI PIN Diodes for the Detection of Blue and UV Wavelengths in a Wide Temperature Range", *ECS Transactions*, vol. 31, n. 1, 2010, pages 199-206.
8. ATLAS User's Manual, SILVACO, 2010.
9. H. Lanyon and R. Tuft, "Bandgap narrowing in moderately to heavily doped silicon", *IEEE Trans. On Electron Devices*, vol. 26, n. 7, 1979, pages 1014-1018.
10. Y. Domae et al, "Improvement of the tolerance to total ionizing dose in SOI CMOS", in *Proc. of IEEE Int. SOI Conference*, 2008, pages 135-136.
11. E. Augendre et al, "On the scalability of source/drain current enhancement in thin film sSOI", *Proc. of ESSDERC*, 2005, pages 301-304.